

一维六方压电准晶中正六边形孔边裂纹的反平面问题*

白巧梅, 丁生虎

(宁夏大学 数学统计学院, 银川 750021)

摘要: 研究了一维六方压电准晶中正六边形孔边裂纹的反平面问题,利用复变函数中的 Cauchy 积分公式,通过构造保角映射函数,在电非渗透型的边界条件下得到了孔边裂纹尖端的应力分布以及场强度因子的解析解.通过数值算例,讨论了正六边形的边长和裂纹长度以及剪应力对场强度因子的影响.

关键词: 一维六方压电准晶; 正六边形孔边裂纹; 复变函数方法; 场强度因子

中图分类号: O346.1

文献标志码: A

DOI: 10.21656/1000-0887.390362

引言

准晶是 1982 年由实验发现,1984 年才首次报道的不同于晶体和非晶体的固体新型材料^[1],这一发现被认为是凝聚态物理和材料科学的一项重大进展.迄今在不同合金中已研制出 200 多种准晶,其中半数以上热力学性能稳定,因而准晶又是一种具有良好应用前景的新型材料.由于准晶存在缺陷^[2],而其缺陷与准晶材料的应用密切相关,所以关于准晶缺陷问题的研究备受关注^[3-4].

近年来,Fan(范天佑)^[5]系统地总结了若干准晶平面弹性与断裂力学问题的复变方法,推导出了一维六方准晶的弹性力学方程,求解了一些简单缺陷问题.马晴和李联合等^[6]研究了八次对称二维准晶 II 型单边裂纹的动力学问题.Guo 和 Lu^[7]研究了一维六方准晶体中椭圆孔产生四裂纹的精确解.邵阳和郭俊宏^[8]研究了一维六方准晶中正方形孔边双裂纹的反平面问题.Liu 和 Yang(刘官厅和杨丽英)^[9]研究了一维六方准晶体中无限多位错与半无限裂纹的相互作用应力场的解析解.高健和刘官厅^[10]研究了一维正方准晶中半无限裂纹问题的解析解.

准晶材料具有独特的物理结构和优越的力学性能,其中压电效应是准晶材料重要的物理性质之一.由于准晶中相位子场的存在,导致准晶压电性能比传统晶体要复杂得多.利用严格算子理论,Li 等^[11]研究了一维六方压电准晶的三维通解.李星等^[12]分析了一维六方压电准晶对称条形体中共线双半无限快速传播裂纹的反平面问题,给出了在电非渗透型与电渗透型两种情况下动态应力强度因子的解析解.Yang 等^[13]研究了一维六方压电准晶体中三个不等裂纹

* 收稿日期: 2018-12-29; 修订日期: 2019-08-30

基金项目: 国家自然科学基金(11762016;11762017;11832014);宁夏自然科学基金(NZ17009)

作者简介: 白巧梅(1994—),女,硕士生(E-mail: 1642721043@qq.com);

丁生虎(1980—),男,教授,博士(通讯作者. E-mail: dshnx2006@163.com).

圆孔的反平面问题,徐文帅等^[14]研究了二维十次对称压电准晶含 Griffith 裂纹的平面问题,由于问题的复杂性,目前关于一维六方压电准晶中正六边形孔边裂纹问题的研究尚未见报道。

本文运用复变函数 Cauchy 积分公式,通过构造保角映射函数研究了一维六方压电准晶中正六边形孔边裂纹的反平面问题,获得了应力强度因子和电位移强度因子的解析解,并用数值算例分析了影响因素与等效场强度因子的变化规律。

1 一维六方压电准晶的基本理论

取坐标轴方向为点群 6 mm 一维六方压电准晶的准周期方向,坐标平面 x_1Ox_2 为垂直于准周期方向的平面,建立直角坐标系.根据文献[5, 15],一维六方压电准晶弹性问题的广义 Hooke 定律、变形几何方程、平衡方程分别为

$$\left\{ \begin{array}{l} \sigma_{11} = C_{11}\varepsilon_{11} + C_{12}\varepsilon_{22} + C_{13}\varepsilon_{33} + R_1w_3 - e_{31}^1E_3, \\ \sigma_{22} = C_{12}\varepsilon_{11} + C_{11}\varepsilon_{22} + C_{13}\varepsilon_{33} + R_1w_3 - e_{31}^1E_3, \\ \sigma_{33} = C_{13}\varepsilon_{11} + C_{13}\varepsilon_{22} + C_{33}\varepsilon_{33} + R_2w_3 - e_{31}^1E_3, \\ \sigma_{12} = \sigma_{21} = 2C_{66}\varepsilon_{12}, \\ \sigma_{13} = \sigma_{31} = 2C_{44}\varepsilon_{31} + R_3w_1 - e_{15}^1E_1, \\ \sigma_{23} = \sigma_{32} = 2C_{44}\varepsilon_{32} + R_3w_2 - e_{15}^1E_2, \\ H_{31} = 2R_3\varepsilon_{31} + K_2w_1 - e_{15}^2E_1, \\ H_{32} = 2R_3\varepsilon_{32} + K_2w_2 - e_{15}^2E_2, \\ H_{33} = R_1(\varepsilon_{11} + \varepsilon_{22}) + R_2\varepsilon_{33} + K_1w_3 - e_{31}^2E_3, \\ D_1 = 2e_{15}^1\varepsilon_{31} + e_{15}^2w_1 + \epsilon_{11}E_1, \\ D_2 = 2e_{15}^1\varepsilon_{32} + e_{15}^2w_2 + \epsilon_{11}E_2, \\ D_3 = e_{31}^1(\varepsilon_{11} + \varepsilon_{22}) + e_{33}^1\varepsilon_{33} + e_{33}^2w_3 + \epsilon_{33}E_3, \end{array} \right. \quad (1)$$

$$\varepsilon_{ij} = \frac{1}{2}(\partial_j u_i + \partial_i u_j), \quad w_j = \partial_j w, \quad E_j = -\partial_j \phi \quad (i, j = 1, 2, 3), \quad (2)$$

$$\sum_{j=1}^3 \partial_j \sigma_{ij} = 0 \quad (i = 1, 2, 3), \quad \sum_{j=1}^3 \partial_j H_{3j} = 0, \quad \sum_{j=1}^3 \partial_j D_j = 0, \quad (3)$$

其中 $\partial_j u_i = \frac{\partial u_i}{\partial x_j}$, σ_{ij} , ε_{ij} , u_i 分别表示声子场的应力、应变与位移分量; H_{ij} , w_j , w 分别表示相位子场的应力、应变与位移分量; E_j , D_j 分别表示电场和电位移; C_{11} , C_{12} , C_{13} , C_{33} , C_{44} , C_{66} 是 6 个声子场弹性常数; K_1 , K_2 是两个相位子场弹性常数; e_{ij}^1 , e_{ij}^2 表示压电常数, ϵ_{11} , ϵ_{33} 表示介电常数; R_1 , R_2 , R_3 是 3 个声子场与相位子场耦合的独立弹性常数; ϕ 表示电势。

当缺陷沿准晶的准周期方向穿透时,材料的几何性质不随准周期方向改变,则有^[16]

$$\partial_3 u_i = 0, \quad \partial_3 w = 0, \quad \partial_3 \sigma_{ij} = 0, \quad \partial_3 H_{ij} = 0, \quad \partial_3 D_i = 0. \quad (4)$$

那么该问题可转化为平面问题和反平面问题,这里只对反平面问题进行讨论.将式(4)代入式(1)~(3),得到声子场、相位子场耦合的反平面弹性问题为

$$\left\{ \begin{array}{l} C_{44}\nabla^2 u_3 + R_3\nabla^2 w + e_{15}^1\nabla^2 \phi = 0, \\ R_3\nabla^2 u_3 + K_2\nabla^2 w + e_{15}^2\nabla^2 \phi = 0, \\ e_{15}^1\nabla^2 u_3 + e_{15}^2\nabla^2 w - \epsilon_{11}\nabla^2 \phi = 0. \end{array} \right. \quad (5)$$

当式(5)的系数行列式不等于零时,可进一步写为

$$\nabla^2 u_3 = 0, \nabla^2 w = 0, \nabla^2 \phi = 0. \tag{6}$$

则此问题归结为求解 3 个调和函数,由复变函数理论^[17]知, u_3, w, ϕ 可表示为 3 个解析函数的实部,即

$$u_3 = \text{Re } \varphi(z), w = \text{Re } \psi(z), \phi = \text{Re } \zeta(z), \tag{7}$$

其中 $z = x_1 + ix_2, i = \sqrt{-1}$.

根据解析函数的性质和 Cauchy-Riemann 方程,由式(1)和式(7)可得

$$\begin{cases} \sigma_{13} - i\sigma_{32} = C_{44}\varphi' + R_3\psi' + e_{15}^1\zeta', \\ H_{31} - iH_{32} = R_3\varphi' + K_2\psi' + e_{15}^2\zeta', \\ D_1 - iD_2 = e_{15}^1\varphi' + e_{15}^2\psi' - \epsilon_{11}\zeta', \end{cases} \tag{8}$$

其中

$$\varphi' = \frac{d\varphi}{dz}, \psi' = \frac{d\psi}{dz}, \zeta' = \frac{d\zeta}{dz}.$$

又由于对任意的 $f(z)$, 有 $\text{Im}f(z) = \frac{1}{2i}(f - \bar{f})$, 则式(8)可化为

$$\begin{cases} \sigma_{32} = \sigma_{23} = -\frac{1}{2i}[C_{44}(\varphi' - \bar{\varphi}') + R_3(\psi' - \bar{\psi}') + e_{15}^1(\zeta' - \bar{\zeta}')], \\ H_{32} = -\frac{1}{2i}[R_3(\varphi' - \bar{\varphi}') + K_2(\psi' - \bar{\psi}') + e_{15}^2(\zeta' - \bar{\zeta}')], \\ D_2 = -\frac{1}{2i}[e_{15}^1(\varphi' - \bar{\varphi}') + e_{15}^2(\psi' - \bar{\psi}') - \epsilon_{11}(\zeta' - \bar{\zeta}')]. \end{cases} \tag{9}$$

当初始条件和边界条件给定时,可以确定 φ, ψ, ζ . 进一步地可确定位移场、应力场以及电位移场.

2 正六边形孔边裂纹问题

如图 1 所示,假设一无限大一维六方压电准晶中包含一正六边形孔边裂纹,裂纹沿准周期方向穿透,长分别为 L_1 和 L_2 , L 表示正六边形孔口裂纹. 在无穷远处有一电场,电极化的方向为准周期方向,受到的电载荷力为 P , 同时在无穷远处还受到沿准周期方向的剪应力 τ .

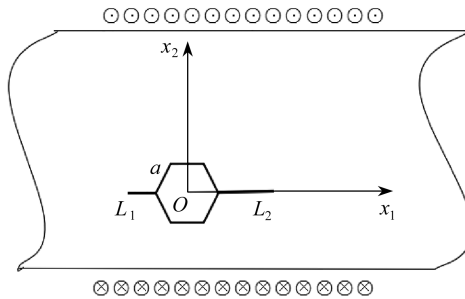


图 1 无限大一维六方压电准晶中正六边形孔边裂纹

Fig. 1 The geometric model for a crack near a regular hexagonal hole in an infinite 1D hexagonal piezoelectric quasicrystal

由线弹性理论分析的结果可知,利用叠加原理,图 1 所示问题可转化为两个线弹性力学

问题的叠加: ① 无裂纹的无限大压电准晶材料, 在无穷远处作用均布力 $\sigma_{32} = -\tau_1, H_{32} = -\tau_2, D_2 = -P$, 其应力强度因子为零, 该问题的解为均场解; ② 具有含边长为 a 的正六边形孔边裂纹的无限大压电准晶材料, 在无穷远处不受力而仅在正六边形孔口以及裂纹表面上作用着均布力 $\sigma_{32} = -\tau_1, H_{32} = -\tau_2, D_2 = -P$. 这两个问题叠加后与无限大压电准晶材料在正六边形孔口以及裂纹表面不受剪应力而在无穷远处作用着均布力 $\sigma_{32} = -\tau_1, H_{32} = -\tau_2, D_2 = -P$ 的情况相同.

问题②为无限大压电准晶在无穷远处不受力只在正六边形孔口以及裂纹表面上作用着 $\sigma_{32} = -\tau_1, H_{32} = -\tau_2, D_2 = -P$ 的情况, 其边界条件可表示为

$$\begin{cases} \sqrt{x_1^2 + x_2^2} \rightarrow \infty : \sigma_{32} = \sigma_{31} = H_{32} = H_{31} = D_2 = 0, \\ (x_1, x_2) \in L : \sigma_{32} = -\tau_1, H_{32} = -\tau_2, D_2 = -P. \end{cases} \quad (10)$$

把式(10)代入式(9)得

$$\begin{cases} C_{44}(\varphi' - \bar{\varphi}') + R_3(\psi' - \bar{\psi}') + e_{15}^1(\zeta' - \bar{\zeta}') = 2\tau_1 i, \\ R_3(\varphi' - \bar{\varphi}') + K_2(\psi' - \bar{\psi}') + e_{15}^2(\zeta' - \bar{\zeta}') = 2\tau_2 i, \\ e_{15}^1(\varphi' - \bar{\varphi}') + e_{15}^2(\psi' - \bar{\psi}') - \epsilon_{11}(\zeta' - \bar{\zeta}') = 2Pi. \end{cases} \quad (11)$$

引入保角变换^[18]

$$z = \omega(\zeta) = R \left(\frac{1}{\zeta} + \frac{1}{15} \zeta^{-5} + \frac{1}{99} \zeta^{-11} + \frac{1}{1377} \zeta^{-17} + \dots \right), \quad (12)$$

其中 $R = 0.9258a$, a 为正六边形的边长.

通过如图 2 所示的变换, 由式(13)可将正六边形孔边裂纹外部区域保角变换到单位圆内部区域

$$z = \omega(\zeta) = R \left(\chi(\zeta^{-1}) + \frac{1}{15} \chi(\zeta^{-1})^5 + \frac{1}{99} \chi(\zeta^{-1})^{11} + \frac{1}{1377} \chi(\zeta^{-1})^{17} \right). \quad (13)$$

在式(13)中, 令 $\zeta = \zeta^{-1}$, 再将单位圆内部的保角变换到单位圆外部, 得到正六边形外部区域到单位圆外部区域的共形映射.

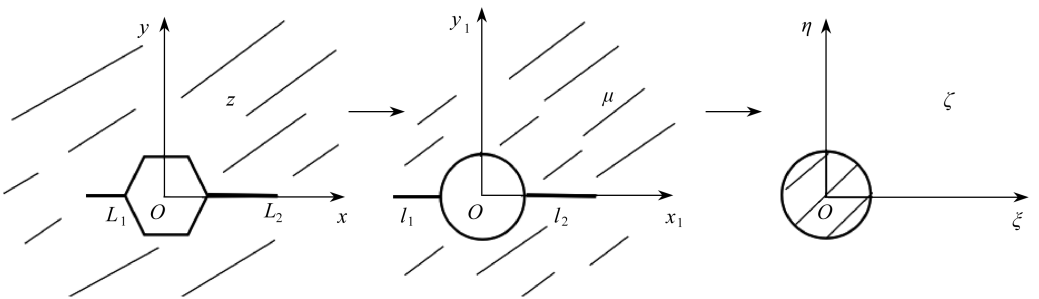


图 2 含正六边形孔边裂纹的平面到单位圆平面的映射

Fig. 2 Mapping of a plane containing double cracks at a regular hexagonal hole to a plane with a unit circle

那么正六边形孔边裂纹外部区域到单位圆内部区域的保角变换函数^[19]为

$$\chi(\zeta) = \frac{1}{4\zeta} \{ \varepsilon_1(1 + \zeta)^2 + \varepsilon_2(1 - \zeta)^2 + \sqrt{(\varepsilon_1^2 - 1)(1 + \zeta)^4 + 2(\varepsilon_1\varepsilon_2 + 1)(1 - \zeta^2)^2 + (\varepsilon_1^2 - 1)(1 + \zeta)^4} \}, \quad (14)$$

其中 $\varepsilon_i = (1 + l_i + (1 + l_i)^{-1})/2, i = 1, 2, l_i$ 为 L_i 经过保角映射后的长度. 保角变换函数式(13)

将物理平面上的区域映射到数学平面上的单位圆内部区域,边界 L 变为 ζ 平面上的单位圆 l ,其中由点的对应关系可得

$$\omega^{-1}(a + L_2) \rightarrow 1, \omega^{-1}(-a - L_1) \rightarrow -1. \tag{15}$$

将式(14)代入式(13)进行 Laurent 级数展开,得到 $\omega(\zeta)$ 的前四项展开式为

$$\omega(\zeta) = b_{-1} \frac{1}{\zeta} + b_0 + b_1 \zeta + b_2 \zeta^2, \tag{16}$$

其中

$$b_{-1} = \frac{R(\varepsilon_1 + \varepsilon_2 + \sqrt{(\varepsilon_1 + \varepsilon_2)^2})}{4}, \tag{17}$$

$$b_0 = \frac{1}{2} R \left(\varepsilon_1 - \varepsilon_2 + \frac{(\varepsilon_1^2 - \varepsilon_2^2)}{\sqrt{(\varepsilon_1 + \varepsilon_2)^2}} \right), \tag{18}$$

$$b_1 = \frac{1}{4} R \left(\varepsilon_1 + \varepsilon_2 + \frac{\sqrt{(\varepsilon_1 + \varepsilon_2)^2} (-8 + \varepsilon_1^2 + 2\varepsilon_1\varepsilon_2 + \varepsilon_2^2)}{(\varepsilon_1 + \varepsilon_2)^2} \right), \tag{19}$$

$$b_2 = \frac{4R(\varepsilon_1 - \varepsilon_2) \sqrt{(\varepsilon_1 + \varepsilon_2)^2}}{(\varepsilon_1 + \varepsilon_2)^3}. \tag{20}$$

令

$$\begin{cases} G_1(\zeta) = \varphi(z) = \varphi(\omega(\zeta)), \\ G_2(\zeta) = \psi(z) = \psi(\omega(\zeta)), \\ G_3(\zeta) = \varsigma(z) = \varsigma(\omega(\zeta)), \end{cases}$$

则有

$$\varphi'(z) = G'_1(\zeta)/\omega'(\zeta), \psi'(z) = G'_2(\zeta)/\omega'(\zeta), \varsigma'(z) = G'_3(\zeta)/\omega'(\zeta). \tag{21}$$

将式(21)代入式(11),整理后将边界上的点 $\zeta = \sigma = e^{i\theta}$ 代入,得到

$$\begin{cases} G'_1(\sigma) - \frac{\omega'(\sigma)}{\omega'(\sigma)} \overline{G'_1(\sigma)} + \frac{R_3}{C_{44}} \left[G'_2(\sigma) - \frac{\omega'(\sigma)}{\omega'(\sigma)} \overline{G'_2(\sigma)} \right] + \\ \frac{e_{15}^1}{C_{44}} \left[G'_3(\sigma) - \frac{\omega'(\sigma)}{\omega'(\sigma)} \overline{G'_3(\sigma)} \right] = \frac{2\tau_1 i}{C_{44}} \omega'(\sigma), \\ \frac{R_3}{K_2} \left[G'_1(\sigma) - \frac{\omega'(\sigma)}{\omega'(\sigma)} \overline{G'_1(\sigma)} \right] + \left[G'_2(\sigma) - \frac{\omega'(\sigma)}{\omega'(\sigma)} \overline{G'_2(\sigma)} \right] + \\ \frac{e_{15}^2}{K_2} \left[G'_3(\sigma) - \frac{\omega'(\sigma)}{\omega'(\sigma)} \overline{G'_3(\sigma)} \right] = \frac{2\tau_2 i}{K_2} \omega'(\sigma), \\ \frac{e_{15}^1}{\epsilon_{11}} \left[G'_1(\sigma) - \frac{\omega'(\sigma)}{\omega'(\sigma)} \overline{G'_1(\sigma)} \right] + \frac{e_{15}^2}{\epsilon_{11}} \left[G'_2(\sigma) - \frac{\omega'(\sigma)}{\omega'(\sigma)} \overline{G'_2(\sigma)} \right] - \\ \left[G'_3(\sigma) - \frac{\omega'(\sigma)}{\omega'(\sigma)} \overline{G'_3(\sigma)} \right] = \frac{2P i}{\epsilon_{11}} \omega'(\sigma). \end{cases} \tag{22}$$

将式(22)两边同乘以 $\frac{d\sigma}{2\pi i(\sigma - \zeta)}$ 后沿边界 l 积分,且 $|\zeta| < 1$,由 Cauchy 积分公式得

$$\begin{cases} G'_1(\zeta) + \frac{R_3}{C_{44}} G'_2(\zeta) + \frac{e_{15}^1}{C_{44}} G'_3(\zeta) = \frac{2\tau_1 i}{C_{44}} \cdot \frac{1}{2\pi i} \int_l \frac{\omega'(\sigma)}{\sigma - \zeta} d\sigma, \\ \frac{R_3}{K_2} G'_1(\zeta) + G'_2(\zeta) + \frac{e_{15}^2}{K_2} G'_3(\zeta) = \frac{2\tau_2 i}{K_2} \cdot \frac{1}{2\pi i} \int_l \frac{\omega'(\sigma)}{\sigma - \zeta} d\sigma, \\ \frac{e_{15}^1}{\epsilon_{11}} G'_1(\zeta) + \frac{e_{15}^2}{\epsilon_{11}} G'_2(\zeta) - G'_3(\zeta) = \frac{2Pi}{\epsilon_{11}} \cdot \frac{1}{2\pi i} \int_l \frac{\omega'(\sigma)}{\sigma - \zeta} d\sigma. \end{cases} \quad (23)$$

式(23)右边的积分,由式(16)可知 $\omega(\zeta)$ 在单位圆内部除一级极点 $\zeta = 0$ 外是解析的,由留数定理可得

$$\frac{1}{2\pi i} \int_l \frac{\omega'(\sigma)}{\sigma - \zeta} d\sigma = \omega'(\zeta) - \left(\frac{b_{-1}}{\zeta} \right)' = b_1 + 2b_2\zeta = F(\zeta). \quad (24)$$

将式(24)代入式(23),进一步化简为

$$\begin{cases} G'_1(\zeta) = 2i \frac{\Delta_1}{\Delta} F(\zeta), \\ G'_2(\zeta) = 2i \frac{\Delta_2}{\Delta} F(\zeta), \\ G'_3(\zeta) = 2i \frac{\Delta_3}{\Delta} F(\zeta), \end{cases} \quad (25)$$

其中

$$\begin{aligned} \Delta &= C_{44}(e_{15}^2)^2 - 2e_{15}^1 e_{15}^2 R_3 + K_2(e_{15}^1)^2 - R_3^2 \epsilon_{11} + C_{44} \epsilon_{11} K_2, \\ \Delta_1 &= e_{15}^1 K_2 P + (e_{15}^2)^2 \tau_1 + \epsilon_{11} K_2 \tau_1 - R_3 \epsilon_{11} \tau_2 - R_3 e_{15}^2 P - e_{15}^1 e_{15}^2 \tau_2, \\ \Delta_2 &= (e_{15}^1)^2 \tau_2 + C_{44} \epsilon_{11} \tau_2 - R_3 \epsilon_{11} \tau_1 + C_{44} e_{15}^2 P - e_{15}^1 e_{15}^2 \tau_1 - e_{15}^1 R_3 P, \\ \Delta_3 &= R_3^2 P + e_{15}^1 K_2 \tau_1 - R_3 e_{15}^1 \tau_2 - R_3 e_{15}^2 \tau_1 + C_{44} e_{15}^2 \tau_2 - C_{44} K_2 P. \end{aligned}$$

将式(25)代入式(21)得

$$\begin{cases} \varphi'(z) = \frac{G'_1(\zeta)}{\omega'(\zeta)} = 2i \frac{\Delta_1}{\Delta} \frac{F(\zeta)}{\omega'(\zeta)}, \\ \psi'(z) = \frac{G'_2(\zeta)}{\omega'(\zeta)} = 2i \frac{\Delta_2}{\Delta} \frac{F(\zeta)}{\omega'(\zeta)}, \\ \varsigma'(z) = \frac{G'_3(\zeta)}{\omega'(\zeta)} = 2i \frac{\Delta_3}{\Delta} \frac{F(\zeta)}{\omega'(\zeta)}. \end{cases} \quad (26)$$

将式(26)代入式(7)和式(9),再利用保角变换的逆映射就可得到 z 平面内应力场和位移场的表达式,由于具体表达过于复杂,故不在此列出。

3 裂尖处的场强度因子

场强度因子是反映裂纹尖端附近应力集中的强弱程度,材料破坏的起点往往是裂尖,所以计算和测定材料的场强度因子非常重要.由文献[5]可得,在 z 平面内裂纹尖端 $z = a + L_2$ 处,对应 ζ 平面内 $\zeta = 1$ 处的场强度因子分别为

$$K_{III}^\sigma = \lim_{\zeta \rightarrow 1} \frac{2\sqrt{\pi} \tau_1 F(\zeta)}{\sqrt{\omega''(\zeta)}} = \sqrt{\pi R} \tau_1 \frac{(\epsilon_1 + \epsilon_2)^2 - 4 + \frac{16(\epsilon_1 - \epsilon_2)}{\epsilon_1 + \epsilon_2}}{\sqrt{(\epsilon_1 + \epsilon_2)^3 + 8(\epsilon_1 - \epsilon_2)}}, \quad (27)$$

$$K_{\text{III}}^H = \lim_{\zeta \rightarrow 1} \frac{2\sqrt{\pi}\tau_2 F(\zeta)}{\sqrt{\omega''(\zeta)}} = \sqrt{\pi R} \tau_2 \frac{(\varepsilon_1 + \varepsilon_2)^2 - 4 + \frac{16(\varepsilon_1 - \varepsilon_2)}{\varepsilon_1 + \varepsilon_2}}{\sqrt{(\varepsilon_1 + \varepsilon_2)^3 + 8(\varepsilon_1 - \varepsilon_2)}}, \quad (28)$$

$$K_{\text{III}}^D = \lim_{\zeta \rightarrow 1} \frac{2\sqrt{\pi}PF(\zeta)}{\sqrt{\omega''(\zeta)}} = \sqrt{\pi RP} \frac{(\varepsilon_1 + \varepsilon_2)^2 - 4 + \frac{16(\varepsilon_1 - \varepsilon_2)}{\varepsilon_1 + \varepsilon_2}}{\sqrt{(\varepsilon_1 + \varepsilon_2)^3 + 8(\varepsilon_1 - \varepsilon_2)}}. \quad (29)$$

为了方便比较,引入等效场强度因子 $k = [K_{\text{III}}^\sigma, K_{\text{III}}^H, K_{\text{III}}^D]^T / (\sqrt{\pi L'} [\tau_1, \tau_2, P]^T)$, 将场强度因子无量纲化,其中 $L' = (L_1 + L_2 + 2a)/2$.

4 数值算例与讨论

观察场强度因子的解析解,发现场强度因子与等效场强度因子、应力、载荷、正六边形边长以及裂纹长度有关,下面分别讨论它们之间的影响规律.

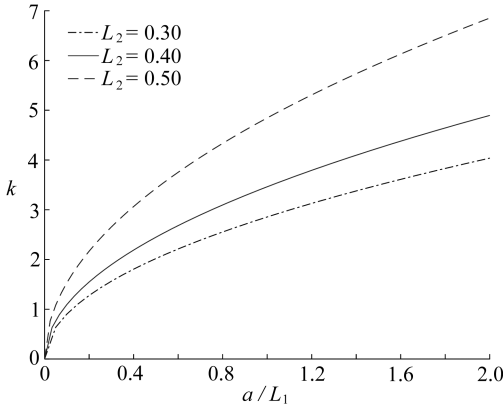


图3 等效场强度因子随正六边形边长的变化
Fig. 3 Variation of the equivalent field intensity factor with the side length of the regular hexagon

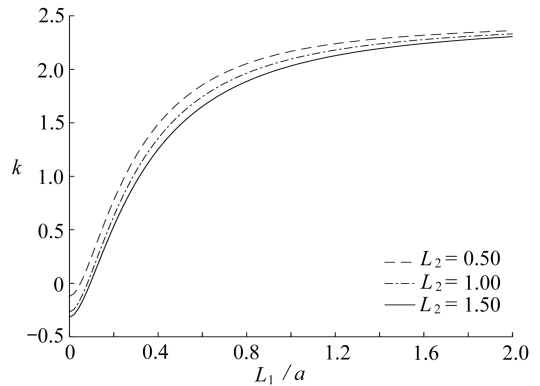


图4 等效场强度因子随裂纹长度的变化
Fig. 4 Variation of the equivalent field intensity factor with the crack length

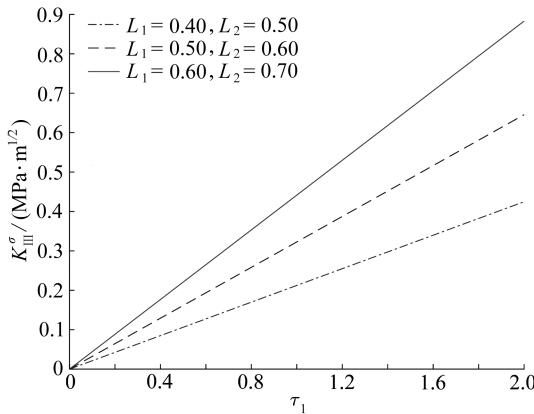


图5 声子场应力强度因子随剪应力 τ_1 的变化

Fig. 5 Variation of the phonon field stress intensity factor with shear stress τ_1

由图3可以得到等效场强度因子与正六边形边长的关系.在裂纹长度 L_1, L_2 不变的情况下,等效场强度因子随着正六边形边长 a 的增大而增大,说明正六边形的边长影响裂纹的扩

展.当正六边形的边长一定时,随着裂纹长度 L_2 的增大,裂纹尖端的等效场强度因子逐渐增大,这与文献[8]的结果一致.

由图4可以得到等效场强度因子与裂纹长度的关系.在正六边形边长不变的情况下,当左裂纹 L_1 的长度不变时,随着右裂纹 L_2 增大等效场强度因子逐渐减小,说明裂纹扩展到一定长度会趋于稳定状态;当左裂纹 L_1 的长度逐渐增大时,右裂纹 L_2 尖端的等效场强度因子先增大后趋于一定值,说明左裂纹的扩展可以减缓右裂纹的扩展.

由图5可以得到剪应力与声子场应力强度因子的关系.在正六边形边长不变的情况下,声子场应力强度因子随着剪应力的增大而增大;同时当剪应力的大小不变时,声子场应力强度因子随着裂纹长度的增大而增大,说明剪应力 τ_1 的增大会促进裂纹的扩展.

5 结 论

本文在电非渗透型的边界条件下借助复变函数方法,解决了一维六方压电准晶中正六边形孔边裂纹的反平面问题,并得到了场强度因子的解析解.从数值结果可以看出,场强度因子随着正六边形边长的增大而增大,左右裂纹互相影响,左裂纹的长度影响右裂纹的扩张,最后剪应力的增大会导致应力强度因子增大.相应地,也可以得到电载荷对场强度因子的影响规律.这些结论为工程的实际应用提供了理论基础与指导意义.

参考文献(References):

- [1] SHECHTMAN D, BLECH I, GRATIAS D, et al. Metallic phase with long-range orientational order and no translational symmetry[J]. *Physical Review Letters*, 1984, **53**(20): 1951-1953.
- [2] ZHANG Z, URBAN K. Transmission electron microscope observations of dislocations and stacking faults in a decagonal Al-Cu-Co alloy[J]. *Philosophical Magazine Letters*, 1989, **60**(3): 97-102.
- [3] LIU G T, GUO R P, FAN T Y. On the interaction between dislocations and cracks in one-dimensional hexagonal quasi-crystals[J]. *Chinese Physics*, 2003, **12**(10): 1149-1155.
- [4] LIU G T, FAN T Y, GUO R P. Governing equations and general solutions of plane elasticity of one-dimensional quasicrystals[J]. *International Journal of Solids and Structures*, 2004, **41**(14): 3949-3959.
- [5] FAN T Y. *The Mathematical Theory of Elasticity of Quasicrystals and Its Applications*[M]. Beijing: Springer-Verlag, 2010.
- [6] 马晴, 王桂霞, 李联合. 八次对称二维准晶 II 型单边裂纹的动力学问题[J]. *应用数学和力学*, 2018, **39**(10): 1180-1188.(MA Qing, WANG Guixia, LI Lianhe. Dynamic problems of mode II cracks in 2D octagonal quasicrystals[J]. *Applied Mathematics and Mechanics*, 2018, **39**(10): 1180-1188.(in Chinese))
- [7] GUO J H, LU Z X. Exact solution of four cracks originating from an elliptical hole in one-dimensional hexagonal quasicrystals[J]. *Applied Mathematics & Computation*, 2011, **217**(22): 9397-9403.
- [8] 邵阳, 郭俊宏. 一维六方准晶中正方形孔边双裂纹的反平面问题[J]. *内蒙古工业大学学报*, 2014, **33**(2): 81-87.(SHAO Yang, GUO Junhong. Anti-plane analysis of double cracks originating from a square hole in one-dimensional hexagonal quasicrystals[J]. *Journal of Inner Mongolia University of Technology*, 2014, **33**(2): 81-87.(in Chinese))
- [9] LIU G T, YANG L Y. Interaction between infinitely many dislocations and a semi-infinite crack

- in one-dimensional hexagonal quasicrystal[J]. *Chinese Physics*, 2017, **26**(9): 280-284.
- [10] 高健, 刘官厅. 一维正方准晶中半无限裂纹问题的解析解[J]. 应用数学和力学, 2015, **36**(9): 945-955. (GAO Jian, LIU Guanting. Analytical solution for problems of 1D orthorhombic quasicrystal with semi-infinite crack[J]. *Applied Mathematics and Mechanics*, 2015, **36**(9): 945-955. (in Chinese))
- [11] LI X Y, LI P D, WU T H, et al. Three-dimensional fundamental solutions for one-dimensional hexagonal quasicrystal with piezoelectric effect[J]. *Physics Letters A*, 2014, **378**(10): 826-834.
- [12] 李星, 霍华颂, 时朋朋. 一维六方压电准晶对称条形体中共线双半无限快速传播裂纹的解析解[J]. 固体力学学报, 2014, **35**(2): 135-141. (LI Xing, HUO Huasong, SHI Pengpeng. Analytic solutions of two collinear fast propagating cracks in a symmetrical strip of one-dimensional hexagonal piezoelectric quasicrystals[J]. *Chinese Journal of Solid Mechanics*, 2014, **35**(2): 135-141. (in Chinese))
- [13] YANG J, LI X, DING S H. Anti-plane analysis of a circular hole with three unequal cracks in one-dimensional hexagonal piezoelectric quasicrystals[J]. *Chinese Journal of Engineering Mathematics*, 2016, **33**(2): 184-198.
- [14] 徐文帅, 杨连枝, 高阳. 二维十次对称压电准晶含 Griffith 裂纹的平面问题[J]. 浙江大学学报(工学版), 2018, **52**(3): 487-496. (XU Wenshuai, YANG Lianzhi, GAO Yang. Plane problems of 2D decagonal quasicrystals of piezoelectric effect with Griffith cracks[J]. *Journal of Zhejiang University (Engineering Science)*, 2018, **52**(3): 487-496. (in Chinese))
- [15] WANG X, PAN E. Analytical solutions for some defect problems in 1D hexagonal and 2D octagonal quasicrystals[J]. *Pramana*, 2008, **70**(5): 911-933.
- [16] 刘官厅, 何青龙, 郭瑞平. 一维六方准晶非周期平面内的平面应变理论[J]. 物理学报, 2009, **58**(S1): 118-123. (LIU Guanting, HE Qinglong, GUO Ruiping. The plane strain theory for one-dimensional hexagonal quasicrystals in aperiodical plane[J]. *Acta Physica Sinica*, 2009, **58**(S1): 118-123. (in Chinese))
- [17] 路见可. 平面弹性复变方法[M]. 武汉: 武汉大学出版社, 2002. (LU Jianke. *Plane Elastic Complex Method* [M]. Wuhan: Wuhan University Press, 2002. (in Chinese))
- [18] 侯祥林, 王家祥, 贾连光. 正六边形孔角裂纹应力强度因子复变函数解[J]. 应用力学学报, 2018, **35**(3): 484-488. (HOU Xianglin, WANG Jiaxiang, JIA Lianguang. Complex variable function solutions of stress intensity factors for cracks emanating from a hexagonal hole in an infinite plane[J]. *Chinese Journal of Applied Mechanics*, 2018, **35**(3): 484-488. (in Chinese))
- [19] 郭俊宏, 刘官厅. 一维六方准晶中具有不对称裂纹的圆形孔口问题的解析解[J]. 应用数学学报, 2007, **30**(6): 1066-1075. (GUO Junhong, LIU Guanting. Analytic solutions of the one-dimensional hexagonal quasicrystals about problem of a circular hole with asymmetry cracks [J]. *Acta Mathematicae Applicatae Sinica*, 2007, **30**(6): 1066-1075. (in Chinese))

An Anti-Plane Problem of Cracks at Edges of Regular Hexagonal Holes in 1D Hexagonal Piezoelectric Quasicrystals

BAI Qiaomei, DING Shenghu

(School of Mathematics and Statistics, Ningxia University,
Yinchuan 750021, P.R.China)

Abstract: The anti-plane problem of cracks near regular hexagonal holes in 1D hexagonal piezoelectric quasicrystals was studied. By means of the Cauchy integral formula in the complex variable functions and through construction of conformal mapping functions, the analytical solutions of stress distribution and field intensity factors at the crack tip near the hole were obtained under the electrically impermeable boundary condition. The effects of the edge length and the crack length of the regular hexagon as well as the shear stress on the field intensity factors were discussed with numerical examples.

Key words: 1D hexagonal piezoelectric quasicrystal; regular hexagonal hole edge crack; complex variable function method; stress intensity factor

Foundation item: The National Natural Science Foundation of China (11762016; 11762017; 11832014)

引用本文/Cite this paper:

白巧梅, 丁生虎. 一维六方压电准晶中正六边形孔边裂纹的反平面问题[J]. 应用数学和力学, 2019, **40**(10): 1071-1080.

BAI Qiaomei, DING Shenghu. An anti-plane problem of cracks at edges of regular hexagonal holes in 1D hexagonal piezoelectric quasicrystals[J]. *Applied Mathematics and Mechanics*, 2019, **40**(10): 1071-1080.